Rapid mechanochemical synthesis of amorphous alloys

Cite as: AIP Advances **7**, 045201 (2017); https://doi.org/10.1063/1.4979890
Submitted: 19 January 2017 • Accepted: 24 March 2017 • Published Online: 04 April 2017

T. D. Hatchard, A. Genkin and M. N. Obrovac

Rapid mechanochemical synthesis of amorphous alloys

T. D. Hatchard, A. Genkin, and M. N. Obrovac[a]
Department of Chemistry, Dalhousie University, Halifax, Nova Scotia B3H 4R2, Canada

(Received 19 January 2017; accepted 24 March 2017; published online 4 April 2017)

A rapid method for preparing amorphous alloys has been developed utilizing a SPEX high energy ball mill. Parameters such as ball size, mass of balls and milling time, were systematically optimized to prepare amorphous alloys quickly. Amorphous alloys previously not thought possible to synthesize by means of SPEX milling were made amorphous by the new method. When applied to the preparation of Sn-Co-C and Si-Fe alloys, the method was found to produce fully amorphous alloys in a matter of hours instead of days or weeks of milling by traditional techniques. Electrochemical performance of the alloys produced by the rapid milling technique in Li cells was found to be the same or superior to alloys produced by the more time consuming methods, confirming their amorphous microstructure. [http://dx.doi.org/10.1063/1.4979890]

I. INTRODUCTION

Mechanical alloying is an important method used to produce nanostructured metals and alloys for a number of applications, including those in the fields of powder metallurgy (e.g. high temperature turbines), magnetic materials, and hydrogen storage. Nanostructured Si and Sn based alloys made by mechanical milling are under intensive study for application in Li-ion batteries, since they can store considerably more Li than conventional graphite negative electrodes.[1,2] During the mechanical alloying process, there is general agreement that the crystallite size of alloys decreases with milling time.[3,4] The final grain size is achieved when there is a balance between dislocation accumulation and dynamic recovery or recrystallization.[3,4] It has further been reported that only high energy impacts will contribute to alloying reactions.[3] Therefore the use of either more small balls or less bigger balls is seen as a tradeoff between impact frequency and impact efficiency.[3] The total strain imparted to the material during milling, rather than the milling energy or collision frequency is also thought to be related to the grain size obtained, as long as the impacts are of a high enough energy to produce plastic deformation, fracturing or cold welding.[3] This implies that many lower energy impacts should eventually produce the same results as a few high energy impacts.

Phase formation during high energy ball milling may be driven by thermodynamics, if the resulting phase is an equilibrium phase of lower energy than the starting materials. However, it is also possible to create non-equilibrium, or metastable, phases by milling. In these cases the driving force for metastable phase formation comes from cumulative dislocation energy stored in the material during milling.[5] The structural complexity of possible equilibrium phases may also play a role in the formation of metastable phases. If there is a structurally simpler metastable state available, then such a phase may be easier to nucleate and form in preference to the equilibrium phase for a given composition.[5]

A high energy SPEX mill is often used for mechanochemical alloying or alloy grain size reduction at the lab scale. In this method a 65 ml sealed cylindrical vial (typically of hardened steel or tungsten

[a]corresponding author: mnobrovac@dal.ca

carbide) containing the precursor powders and milling media (typically hardened steel, stainless steel or tungsten carbide balls of uniform size) are oscillated through an arc of about 10 cm in length at a frequency of about 16.5 Hz. Alloying takes place when powder becomes trapped in the ball-wall or ball-ball collisions that occur inside the vial. This method has not been completely optimized for producing nano-structured or amorphous alloys.[3] Typically SPEX milling is conducted in a mode that maximizes impact energy, as it is widely believed that low impact energy cannot induce alloying.[3] Therefore milling conditions that employ a few large (5 - 8 g, 1.3 - 1.5 cm diameter[6–10]) balls are widely used.[3] Very nice results can sometimes be achieved under these conditions[10,11] but the resulting materials can also be microcrystalline as opposed to amorphous or nano-structured.[6,8] Recently it has been shown that low energy milling can result in the formation of alloys that are more amorphous than SPEX milled alloys.[12] In contrast to SPEX milling in which products can reach a steady state in hours/days, steady state conditions are typically achieved only after weeks of roller milling.[12–14]

It occurred to us that the low energy milling regime was not fully explored for the SPEX milling method because it is generally believed that only high energy impacts contribute to alloying, as discussed above. By making the ball size substantially smaller than what is typically used, the impact energy in a SPEX mill could be greatly reduced. Because of the faster impact frequency of the SPEX mill, the use of many small balls should result in highly efficient low energy milling. Here this method is explored and optimized by investigating the effect of milling parameters on the amorphization of crystalline Si powder. The optimized method is then used to make Si and Sn-based amorphous alloys for use as negative electrode materials in Li-ion cells. The microstructure of these alloys is critical to their electrochemical performance.[1,2,9,15] The existence of crystalline species will induce 2-phase coexistence during lithiation, resulting in immense stress along phase boundaries, crack propagation, electrical disconnection of alloy particles and, ultimately, severe capacity fade during charge/discharge cycling.[1,2] The electrochemical properties of such alloys are extremely sensitive to their microstructure and can be more sensitive than what is detectable by x-ray diffraction.[8,15] Therefore, the electrochemical performance of these alloys in addition to their x-ray diffraction patterns were used to evaluate the effectiveness of milling methods in producing nanocrystalline/amorphous alloys.

II. EXPERIMENTAL

A. Si grain size reduction

Varying amounts of Si powder (Sigma Aldrich, 325 mesh, 99%) were loaded into 65 ml hardened steel vials (SPEX) with various amounts of different sized 440C stainless steel balls (Thomson Linear Motion). The sample vials were sealed in an Ar atmosphere. Duplicate samples were milled simultaneously in a SPEX 8000D dual mixer mill, with the vial positions being switched at 2 hour intervals during milling. Table I summarizes the milling conditions for each experiment. After milling, the Si powder was recovered from the vials and powder x-ray diffraction (XRD) patterns were collected. When the ball diameter was 3.2 mm or larger, the powder was recovered directly after milling by opening the vial in air and dumping out the sample. When the ball diameter was less than 3.2 mm, too much sample was stuck to the balls to allow an adequate sample recovery. In these cases, the vial was approximately half filled with 100 % ethanol and then milled for an additional 2 – 5 minutes. The vial contents were then poured into a sieve and the ethanol-powder mixture was collected in a pan. The ethanol was then evaporated in a solvent oven at 120 °C in air, in order to recover the Si sample. No difference was found by XRD in samples that were recovered with ethanol versus those that were recovered without the use of a solvent.

B. $Sn_{30}Co_{30}C_{40}$ alloy preparation

Stoichiometric amounts of Sn powder (Alfa Aesar, 99.8%, -325 mesh), Co powder (Aldrich Chemical Company, 99.8%, < 2 um) and MAG-E graphite (Hitachi, average size of 20 μm) were loaded into a 65 ml hardened steel vial (SPEX) with a total sample volume of 0.5 ml. 180 g of 1.6 mm 440C stainless steel balls (Thomson Linear Motion) were added to the vial which was sealed in

TABLE I. Summary of experiments used to determine optimal SPEX milling parameters for the rapid amorphization of Si powder. The sample volume was determined from the bulk density. The grain size and % unmilled Si values are averaged over at least four replicate experiments, with the quantities in brackets indicating standard deviations in the last digit.

Sample	Sample Volume (ml)	Ball Diameter (mm)	Total Ball Mass (g)	Milling Time (h)	Milled Si Grain Size (nm)	Unmilled Si (atomic %)
1	0.50	11	11	4		
2	0.50	11	22	4	9.8(3)	2.2(3)
3	0.50	11	33	4	9.8(2)	2.2(3)
4	0.50	11	45	4	9.6(2)	2.1(3)
5	0.50	6.4	45	4	9.0(2)	1.8(2)
6	0.50	6.4	90	4	8.6(3)	1.5(3)
7	0.50	6.4	135	4	7.9(2)	1.7(2)
8	0.50	6.4	135	4	7.9(2)	1.8(2)
9	0.50	3.2	135	4	7.2(1)	5(2)
10	0.50	6.4	180	4	7.0(2)	1.4(4)
11	0.50	3.2	180	4	8(2)	8(3)
12	0.50	2.4	180	4	4.88(6)	0.8(1)
13	0.50	1.6	180	4	4.2(4)	1.1(3)
14	0.50	11	180	4	7.9(5)	1.4(3)
15	0.50	1.6	180	1	5.0(4)	2.0(2)
16	0.50	1.6	180	2	4.5(1)	1.24(2)
17	0.50	1.6	180	8	4.2(4)	1.0(3)
18	0.50	0.4	180	4	1.11(8)	0.2(1)
19	0.75	1.6	180	4	4.4(7)	2.8(2)
20	0.50	0.6	180	4	3(2)	0.7(3)
21	0.49	0.6	180	4	4.0(4)	0.89(8)

an Ar atmosphere. The sample was milled in a SPEX 8000M mixer mill for 4 hours with the vial being rotated 180° after 2 hours. The sample was then recovered with the aid of ethanol, as described above.

C. $Si_{85}Fe_{15}$ alloy preparation

Stoichiometric amounts of Si powder (Sigma Aldrich, 99%, -325 mesh) and Fe powder (Aldrich Chemical Company, 99.9+%, -325 mesh) were loaded into a 65 ml hardened steel vial (SPEX) with a total sample volume of 0.5 ml, based on bulk density. 180 g of 1.6 mm 440C stainless steel balls (Thomson Linear Motion) were added to the vial which was sealed in an Ar atmosphere. The sample was milled in a SPEX 8000M mixer mill for 4, 8 or 16 hours with the vial being rotated 180° after every 2 hour period. The sample was then recovered with the aid of ethanol, as described above. Samples were also prepared under the same conditions with 8 hours milling time, excepting two 11 mm diameter balls were used.

$Si_{85}Fe_{15}$ was also prepared by roller milling. A total of 5 ml of stoichiometric amounts of Si and Fe powder were loaded into a 16 cm diameter hardened steel roller mill vial with 2.3 kg of 6.4 mm diameter 440C stainless steel balls (Thomson Linear Motion). The vial was sealed under Ar and milled for 5 weeks at a rotation speed that maximized the impact noise of the balls with the vial wall (approximately 80% critical speed). At 1 week intervals, the vial was opened under Ar and a small sample was removed for XRD measurements.

D. Materials characterization

XRD patterns were collected with a Rigaku Ultima IV diffractometer equipped with a diffracted beam graphite monochromator and using Cu K-alpha radiation. Room temperature ^{119}Sn Mössbauer effect spectroscopy was conducted with a Wissel System II constant-acceleration spectrometer using a $Ca^{119m}SnO_3$ source. The velocity scale was referenced to room temperature $CaSnO_3$.

E. Electrode preparation

$Sn_{30}Co_{30}C_{40}$ electrodes were made by combining $Sn_{30}Co_{30}C_{40}$ powder, lithium polyacrylate binder (LiPAA) (35 wt % solution of 250,000 MW polyacrylic acid solution (Aldrich) neutralized with $LiOH{\cdot}H_2O$ (98%, Aldrich)) and carbon black (Super C, Imerys Graphite & Carbon) in a 80:12:8 weight ratio. Distilled water was added to form a slurry. $Si_{85}Fe_{15}$ electrodes were prepared by mixing $Si_{85}Fe_{15}$ powder with polyimide (PI) (20 % solution in NMP, PI2555, HD MicroSystems) and carbon black in a 90:2:8 weight ratio. N-methyl-2-pyrrolidone (Sigma Aldrich, anhydrous 99.5%) was added to form a slurry. Both slurries were mixed for one hour in a Retsch PM200 planetary mill at 100 rpm with four 13 mm tungsten carbide balls and then spread onto copper foil with a 0.1 mm doctor blade. Coatings with LiPAA binder were dried in air at 90 °C for one hour, then under vacuum at 90 °C overnight with no further air exposure. Coatings with PI binder were dried in air for 1 hour at 120 °C and cut into 1.3 cm disks and then heated under Ar for 3 hours at 600 °C with no further air exposure.

F. Coin cell preparation

Circular electrodes with a diameter of 1.3 cm were cut from the dried electrodes and used as cathodes in Li half cells. Typical active material loadings were about 2.5 – 3.0 mAh/cm^2 for $Sn_{30}Co_{30}C_{40}$ electrodes and 8.0 – 10.0 mAh/cm^2 for $Si_{85}Fe_{15}$ electrodes. Coin cells were assembled in an argon-filled glove box. Lithium metal foil was used as the counter electrode. Two layers of Celgard 2301 were used as separators. 1M $LiPF_6$ in a solution of ethylene carbonate, diethyl carbonate and monofluoroethylene carbonate (EC/DEC/FEC; 3:6:1 by volume, all battery grade, BASF) were used as electrolyte. Coin cells were cycled using a Maccor Series 4000 Automated Cycler. $Si_{85}Fe_{15}$ electrodes were cycled with voltage limits of 0.005 – 1.5 V with a rate of C/10 and a C/40 trickle discharge at 0.005 V for the first cycle. For the second and subsequent cycles the voltage limits were 0.005 – 0.900 V and cells were cycled at a rate of C/4 with a C/20 trickle discharge at 0.005 V. $Sn_{30}Co_{30}C_{40}$ electrodes were cycled between limits of 0.005 – 2.5 V at a rate of C/10 with a C/20 trickle discharge at 0.005 V for two cycles and then between limits of 0.005 – 1.2 V at a rate of C/5 with a C/10 trickle discharge at 0.005 V, to match the cycling parameters for similar electrodes in Reference 12.

III. RESULTS AND DISCUSSION

A. Si grain size reduction

Low energy milling may be achieved using a SPEX mill by replacing a few large balls with several small balls. The high collision rate imparted by the SPEX mill's motion should result in accelerated alloy formation. We will show below that this is indeed possible. In order to optimize SPEX milling for amorphization of Si alloys, SPEX milling of crystalline Si powder was performed under a number of different conditions. The conditions were optimized in order to minimize the Si grain size in the shortest period of time. The parameters of the experiments conducted are summarized in Table I, with each entry in the table representing a set of at least four replicate experiments. Grain size was determined using the Scherrer equation applied to the Si (111) diffraction peak. XRD patterns were fit from 25° to 32° using Pseudo-Voigt peak shape functions and a linear background. It was found that two phases were required to describe the collected data. One phase corresponded to un-milled crystalline Si and the other to milled Si with a lower grain size. The peak parameters for the un-milled phase were fixed to be those from the (111) peak of pure un-milled crystalline Si powder. Only the un-milled Si peak area was allowed to vary in subsequent fits. The peak width, shape, position and area of the milled Si peak were all allowed to vary. In this way, the degree of milling achieved could be monitored by tracking the full width at half maximum (FWHM) of the 'milled' Si peak as well as tracking the amount of 'un-milled' Si in the sample (represented by the relative area of the un-milled Si (111) peak). In general, the amount of un-milled Si was quite low (usually less than 2 atomic %), so the FWHM of the (111) peak for the milled Si was the main indicator for success in crystallite size reduction. An example of the fitting technique is shown in Figure 1, with the contributions of both Si phases, the background, the total fit and the collected data shown.

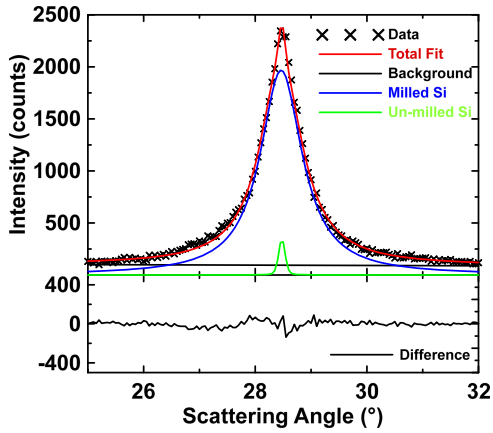

FIG. 1. Example of the fitting technique used for a sample of SPEX milled Si powder (Sample 3, Table I) showing the contribution of the amorphous and un-milled crystalline Si phases, the background, total fit and the collected data.

Figure 2 shows a plot of the Si grain size versus milling time for a fixed sample size (0.5 ml or 1.165 g), ball size (1.6 mm) and ball loading (180 g). The largest grain size reduction occurs during the first 4 hours of milling. The most important parameters affecting Si grain size reduction were the ball diameter, and the ball and sample loading. Figure 3 shows a plot of the Si grain size versus ball diameter for 0.5 ml samples that were milled for 4 hours. The ball loading (in grams) used for each sample is indicated in the figure. At all ball diameters the Si grain size is reduced as the ball loading increases. The Si grain size decreases with decreasing ball size, with a sharp decrease when ball diameter drops below 2 mm. The data points with the smallest ball diameters are for stainless steel shot. This shot has a size range of 20 to 40 mesh or 425 to 850 μm. With this small diameter shot, the Si particle size is greatly reduced. However, a large amount of iron contamination was noticed in the samples, with these samples actually becoming ferromagnetic. This may be due to small size/high surface area of the shot or because of its irregular shape, as opposed to regular spherical bearings.

Figure 4 shows XRD patterns of 0.5 ml of Si powder milled 4 hours with 180 g of 0.4 mm stainless steel shot or 1.6 mm stainless steel balls. The XRD pattern of the powder milled with 1.6 mm balls has broad XRD peaks characteristic of amorphous Si, but also contains some narrower XRD peaks, corresponding to nanocrystalline Si with a grain size of about 7 nm (according to the Scherrer equation applied to the Si (111) peak). The Si sample milled using shot contains no nanocrystalline Si. However other peaks are present that arise from nanocrystalline Fe and $FeSi_2$ phases. It is clear that although reducing milling media size increases the rate of amorphization, it also increases Fe contamination. Further improvements may be made by using other milling media, e.g. Al_2O_3, to avoid contamination.

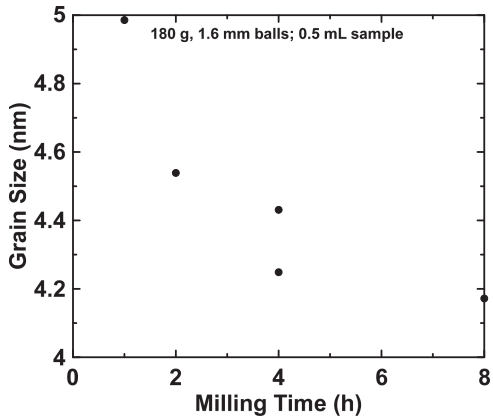

FIG. 2. Grain size versus milling time for 0.5 ml (1.165 g) Si powder loading, with 180 g of 1.6 mm diameter stainless steel balls.

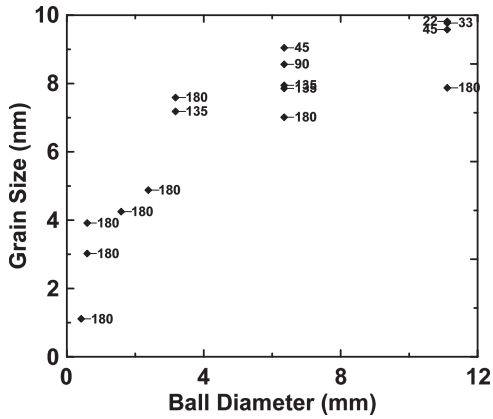

FIG. 3. Plot of average grain size versus ball diameter for all 0.5 ml sample sets that were milled for 4 hours with various ball loadings, as indicated in grams.

From the results above, the optimum milling conditions for Si grain size reduction are those having a maximum number of balls and a minimum ball diameter, depending on what amount of Fe contamination is deemed acceptable. We chose a 0.5 ml sample volume (based on bulk density) and 180 g as the optimum amount of balls, as more than this would limit the free motion of the balls during milling. To avoid Fe contamination, the ball size was chosen to be 1.6 mm, which is the smallest size of hardened stainless steel balls that we can economically obtain. ICP analysis of Si samples milled under these conditions showed that they contained 0.7 - 1 atomic % iron impurity, which was acceptable for our purposes (< 2 atomic %). These conditions will be termed here as optimized SPEX milling conditions. The optimized SPEX milling conditions found here are surprising, since it is generally believed that a higher ball mass is required for rapid milling. For instance, Gauthier et al. ball milled Si powder using conventional SPEX milling conditions with large steel balls and only achieved an average grain size of 10 nm after 20 hours milling time.[9] Here, our optimized SPEX milling method results in an average Si grain size that is less than half of this in only 4 hours. We are not aware of any other reports of SPEX milling under similar conditions.

The use of these optimized SPEX milling conditions to synthesize amorphous alloys is discussed below. It was hoped that applying these conditions would lead to the production of nano-structured or amorphous alloys at the lab scale in a matter of hours, as opposed to the tens of hours required by conventional SPEX milling or days or weeks needed for mechanical attrition or roller milling. This method was evaluated by synthesizing amorphous alloys for use as negative electrodes in Li-ion

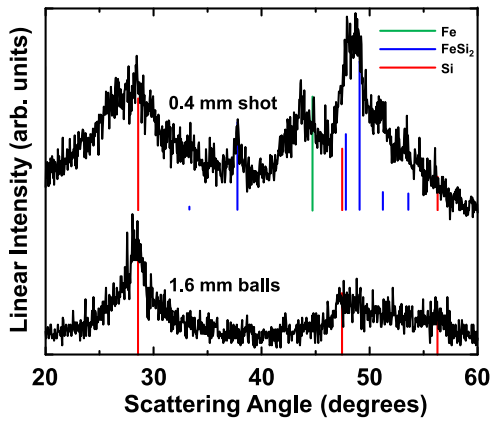

FIG. 4. XRD patterns of 0.5 ml Si powder milled with 180 g of 0.4 stainless steel shot or 1.6 mm stainless steel balls. Vertical lines indicate the positions and relative intensities of Fe, $FeSi_2$, and Si phases.

batteries. Since the microstructure of these materials significantly effects their electrochemical performance,[1] such alloys are ideal for evaluating the effectiveness of our rapid SPEX milling conditions for making alloys with an amorphous microstructure.

B. Optimized SPEX milling of SnCoC alloys

Amorphous SnCoC alloys have been widely investigated as a possible alloy anode for Li-ion batteries. They can be made in the amorphous state by sputtering or by utilizing low energy ball milling for long periods of time (i.e. > 1 week).[12] Traditional methods of making these alloys (a few large milling balls in each SPEX vial) using Sn, Co and C powder precursors cannot produce fully amorphous alloys. Instead, only nanocrystalline alloys with grain sizes of about 14 nm are

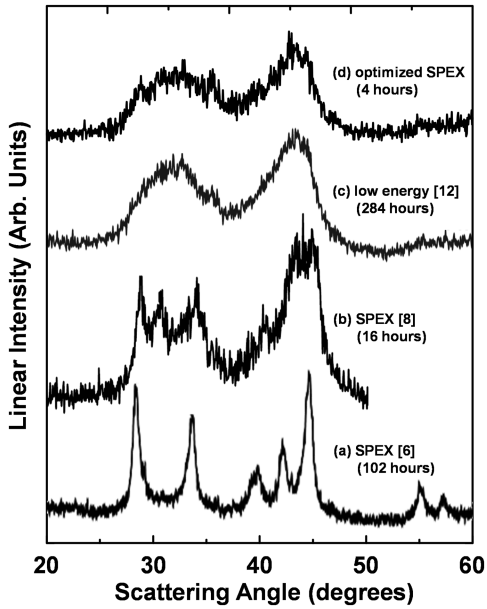

FIG. 5. XRD patterns $Sn_{30}Co_{30}C_{40}$ prepared (a) SPEX milling Sn, Co, C powders with a few large balls (XRD pattern reprinted with permission from Hassoun *et al.,* Electrochem. Commun. **9**, 2075-2081 (2007). Copyright 2007 Elsevier.), (b) SPEX milling $CoSn_2$, Co and C powders with a few large balls (XRD pattern reprinted with permission from Ferguson *et al.*, Electrochem. Commun. **10**, 25-31 (2008). Copyright 2008 Elsevier.), (c) roller milling Sn, Co, C powders for 213 hours (XRD pattern reprinted with permission from J. Ferguson *et al.*, J. Alloys Compd. **595**, 138-141 (2014). Copyright 2014 Elsevier.), and (d) Sn, Co, C powders milled for four hours with the optimum SPEX milling conditions described here.

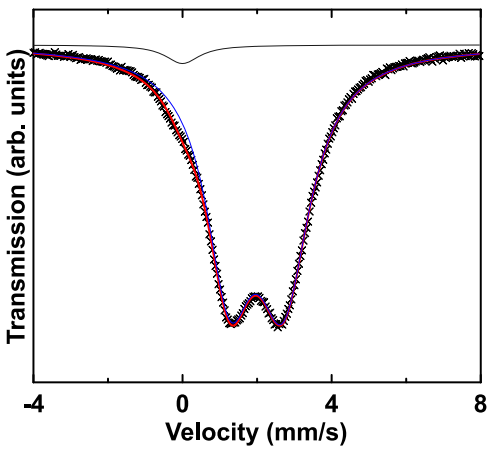

FIG. 6. Room temperature ^{119}Sn Mössbauer effect spectra of $Sn_{30}Co_{30}C_{40}$ prepared by milling Sn, Co, C powders in a SPEX mill for four hours with the optimum SPEX milling conditions described here. The spectral components are described in Table II: CoSn (blue), SnO_2 (black), and total fit (red). The velocity scale is measured relative to $CaSnO_3$.

TABLE II. ^{119}Sn Mössbauer effect hyperfine parameters for the spectra shown in Fig. 6. δ is the center shift relative to $CaSnO_3$ and Δ is the quadrupole splitting. The relative area of each spectral component is indicated.

Component	δ (mm/s)	Δ (mm/s)	Area (%)
CoSn	1.98	1.45	97
SnO_2	0	-	3

produced with clear diffraction peaks from the CoSn phase, even after 102 hours of milling,[6] as shown in Figure 5(a). A reduction in grain size can be achieved when $CoSn_2$, Co and C are used as precursors, shown in Figure 5(b), but SPEX milling with a few large balls could not produce a fully amorphous $Sn_{30}Co_{30}C_{40}$ phase even after 16 hours of milling, with nanocrystalline peaks from Sn-Co intermetallic alloys still being apparent in the XRD pattern. To achieve fully amorphous $Sn_{30}Co_{30}C_{40}$, Ferguson et al. employed a low energy roller milling method, with a long milling time of 284 hours for Sn, Co and C precursor powders,[12] as shown in Figure 5(c).

We used the optimized SPEX milling conditions described above (0.5 ml sample, 180 g 1.6 mm stainless steel balls) to prepare $Sn_{30}Co_{30}C_{40}$ alloy from Sn, Co and C powder precursors. This method produced a fully amorphous alloy in only 4 hours. An XRD pattern of the obtained alloy is shown in Figure 5(d). The XRD pattern is similar to that obtained by Ferguson et al. after 284 hours of low energy milling.[12] A Mössbauer spectrum of the $Sn_{30}Co_{30}C_{40}$ alloy is also shown in Figure 6, with fitting results shown in Table II. The spectrum is composed of a doublet with a center shift and quadrupole splitting that are characteristic of amorphous CoSn grains in a carbon matrix and a small singlet at 0 mm/s corresponding to the presence of a small SnO_2 impurity.[16] These results are consistent with those of Ferguson et al., who found that out of a series of $(Sn_xCo_{1-x})_{60}C_{40}$ samples prepared by mechanical attrition only the $Sn_{30}Co_{30}C_{40}$ composition had a Mössbauer spectrum that consisted of one CoSn doublet component. All other compositions in this series had spectra exhibiting multiple Sn-Co and Sn-Co-C phases.[16] Therefore our SPEX method achieved the same microstructure and comprised the same CoSn phase as prepared by Ferguson, except in about 70 times less milling time.

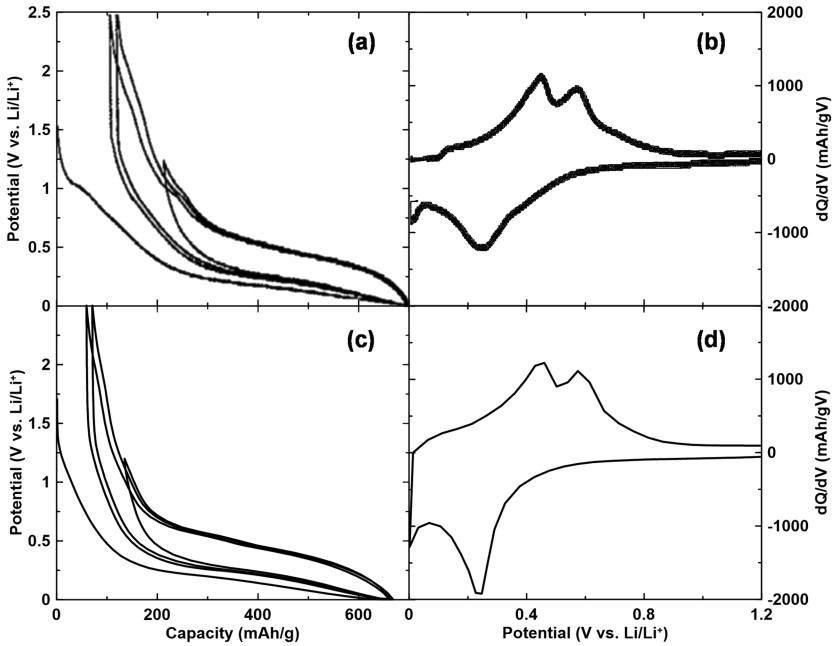

FIG. 7. Voltage and cycle 3 differential capacity curves, respectively, of $Sn_{30}Co_{30}C_{40}$ prepared from Sn, Co, and C powders by (a,b) roller milling 213 hours (Voltage and differential capacity curves reprinted with permission from Ferguson *et al.* , J. Alloys Compd. **595**, 138-141 (2014). Copyright 2014 Elsevier.), and (c,d) milled for four hours with the optimum SPEX milled conditions described here.

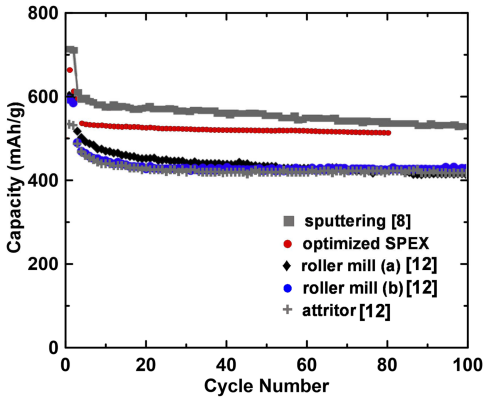

FIG. 8. Cycling performance of $Sn_{30}Co_{30}C_{40}$ prepared from Sn, Co, and C powders by sputter deposition (Cycling data reprinted with permission from Ferguson *et al.*, Electrochem. Commun. **10**, 25-31 (2008). Copyright 2008 Elsevier.), milling for four hours with the optimum SPEX milled conditions described here, and roller milling for 213 hours or 284 hours. (Cycling data reprinted with permission from Ferguson *et al.*, J. Alloys Compd. **595**, 138-141 (2014). Copyright 2014 Elsevier.)

Even more startling is that it was previously believed that the synthesis of amorphous SnCoC alloys was not achievable by SPEX milling, especially when Sn, Co, and C precursors were employed.[6,12] It is clear that the optimized SPEX milling conditions developed here are far superior to those used in previous investigations.

Further information about $Sn_{30}Co_{30}C_{40}$ alloy microstructure can be obtained from its electrochemical performance in Li half cells. Figure 7 shows the voltage curves and differential capacity curves in Li half cells of $Sn_{30}Co_{30}C_{40}$ alloys prepared from Sn, Co and C precursors by roller milling for 284 hours (Reference 12) and by the optimized SPEX milling method for 4 hours. The voltage curves are nearly identical, except that the sample made by the optimized SPEX milling process has much lower irreversible capacity and does not show features above 1 V. The higher irreversible capacity and these extra features in the voltage curve of the roller milled sample were attributed to "electrode processing."[12] The differential capacity curves of both materials are nearly identical, and contain no sharp peaks indicative of 2-phase regions arising from crystalline phases. Figure 8 shows the cycling performance of both materials. Also shown is the cycle performance of $Sn_{30}Co_{30}C_{40}$ obtained by sputtering and by attritor and roller milling. The optimized SPEX milled sample prepared here in 4 hours has higher capacity and much better cycling characteristics than the samples reported in Reference 12 that were attritor milled for 16 hours or roller milled for over 200 hours. In fact the capacity approaches that of sputtered $Sn_{30}Co_{30}C_{40}$. It is believed that higher capacity in Sn-Co-C alloys is indicative of a smaller grain size.[8] Therefore, this suggests that using the optimized SPEX milling method for 4 hours has achieved a smaller grain size than can be produced by roller milling in 284 hours, and, furthermore, that the grain size may approach that achieved by sputtering.

C. Optimized SPEX milling of Si-Fe alloys

Si based alloys are very widely studied for use as anode materials in Li-ion batteries due to the very high specific capacity of Si. To evaluate the optimized SPEX milling method for use in making Si alloys, $Si_{85}Fe_{15}$ alloys were prepared from Si and Fe powders by roller milling and by the rapid SPEX milling technique described here. Alloys of this composition are expected to comprise elemental Si and Si-Fe intermetallic alloys.[17] Figure 9(a) shows the XRD pattern of $Si_{85}Fe_{15}$ alloy made by roller milling for 840 hours. The XRD pattern comprises nanocrystalline iron silicide phases and a small peak at about 44°, which corresponds to Fe metal. This indicates that either some starting materials are not being incorporated into the alloy or that there is iron contamination from the milling vial and balls. No peaks from elemental Si are visible, indicating that this phase is amorphous. $Si_{85}Fe_{15}$ alloys were also prepared by SPEX milling Fe and Si powders under typical conditions with large milling balls: 0.5 ml sample volume milled for 8 hours with two 11 mm balls. The resulting XRD pattern is shown in Figure 9(b). In addition to peaks from Si-Fe intermetallic phases, large XRD peaks from

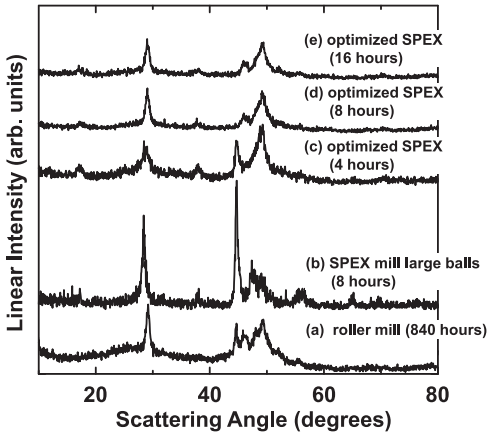

FIG. 9. XRD patterns of $Si_{85}Fe_{15}$ prepared by (a) roller milling for 840 hours, (b) SPEX milling with a few large balls for 8 hours, and milling with the optimum SPEX milling conditions described here for (c) 4 hours, (d) 8 hours, and (e) 16 hours.

crystalline Si and Fe are present. Most of the sample appears to be unalloyed after 8 hours milling under these conditions.

Figures 9(c–e) show the XRD patterns of $Si_{85}Fe_{15}$ alloys made by using optimized SPEX milling conditions. After 4 hours of milling, the XRD pattern mostly corresponds to Si-Fe intermetallic phases, however there is a peak at 44° corresponding to an Fe impurity. This is similar to the sample produced by roller milling after 840 hours. After 8 hours the XRD pattern corresponds to only Si-Fe phases. Any elemental Si present is amorphous. The XRD pattern does not change when the sample was SPEX milled under the same conditions for 16 hours. This shows that the optimized SPEX milling method was able to reproduce amorphous alloys in hours that could not be made under typical SPEX milling conditions or even by several weeks of roller milling.

Figure 10(a) and (b) show the voltage curves for the $Si_{85}Fe_{15}$ alloys prepared by roller milling for 840 hours and optimized SPEX milling for 16 hours. Both voltage curves have smooth features and do not show any evidence of $Li_{15}Si_4$ formation, which is indicative of nanocrystalline Si that is bound to an inactive phase.[17] The optimized SPEX milled sample has lower irreversible capacity, lower voltage polarization (348 mV for the roller milled sample versus 327 mV for the SPEX milled sample) and less evidence of nucleation and growth during the initial lithiation. All these are desirable traits and may arise from smaller grain size. Figure 11 shows the cycling performance of the cells shown in Figure 10. The roller milled $Si_{85}Fe_{15}$ alloy sample has a first discharge capacity of about 1500 mAh/g, reversible capacity of about 800 mAh/g. After this large initial irreversible capacity loss, the alloy has good capacity retention for the first 50 cycles. The 16 hour optimized SPEX milled $Si_{85}Fe_{15}$ alloy sample has a higher discharge capacity (< 1600 mAh/g) and a substantially higher reversible capacity (~ 1200 mAh/g) than the roller milled sample. Good cycling characteristics are also achieved in 50 cycles, but with much less irreversible capacity loss. This represents another example of optimized

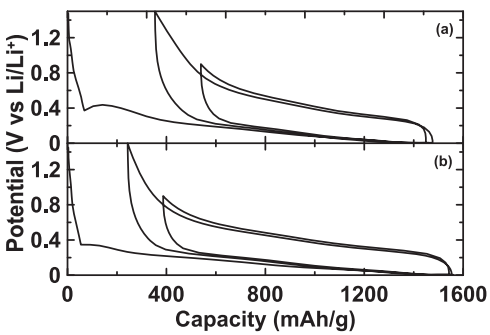

FIG. 10. Voltage curves of $Si_{85}Fe_{15}$ prepared by (a) roller milling for 5 weeks, and (b) milling with the optimum SPEX milling conditions described here for 16 hours.

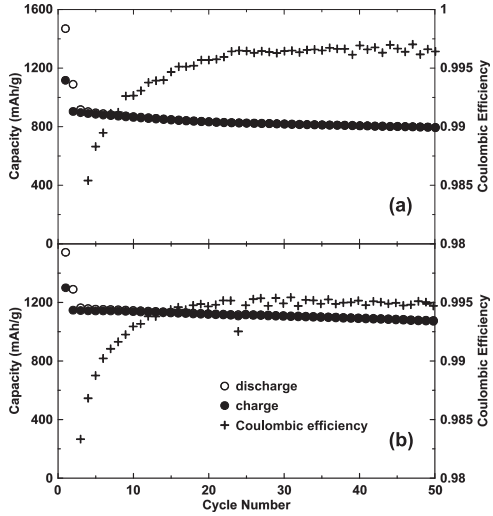

FIG. 11. Cycling performance of $Si_{85}Fe_{15}$ prepared by (a) roller milling for 5 weeks, and (b) milling with the optimum SPEX milling conditions described here for 16 hours.

SPEX milling resulting in the synthesis of an alloy with greatly superior cycling characteristics than one made by roller milling, and in a fraction of the time.

IV. CONCLUSION

A method of rapidly making highly amorphous alloys by SPEX milling was developed. It was found that the rate of amorphization and alloy formation increased with lower ball diameter and a larger amount of balls. This is in contrast to the small number of larger balls typically used for SPEX milling. An increase in iron contamination was observed as the ball size was reduced. Therefore amorphization rate must be balanced with iron contamination when choosing ball size. The optimized method was used to prepare amorphous Sn-Co-C and amorphous/nanocrystalline Si-Fe alloys for use as negative electrodes in Li cells. Such alloys could not be made by using typical SPEX milling conditions, but could be made by roller milling, but only after 284 - 840 hours. By using a large number of small balls, samples could be made by SPEX milling in only 4-16 hours that were superior in microstructure to roller milled samples, as indicated by improved electrochemical performance. SPEX milling in this regime allows alloys to be synthesized with a higher degree of alloying and a higher amorphization than possible by typical SPEX milling conditions, and in a short amount of time. This should enable researchers to speed their investigations of amorphous or nanostructured alloy materials.

ACKNOWLEDGMENTS

The authors would like to thank Dr. Richard Dunlap for assistance with the analysis of Mössbauer spectra. The authors acknowledge funding from NSERC and 3M Canada under the auspices of the Discovery Grants and Industrial Research Chair Programs.

[1] M. N. Obrovac and V. L. Chevrier, Chem. Rev. **114**, 11444 (2014).
[2] N. Mahmood, T. Tang, and Y. Hou, Adv. Energy Mater. **1** (2016).
[3] D. L. Zhang, Prog. Mater. Sci. **49**, 537 (2004).
[4] C. C. Koch, Nanostructured Mater. **9**, 13 (1997).
[5] P. Y. Lee and C. C. Koch, J. Mater. Sci. **23**, 2837 (1988).
[6] J. Hassoun, G. Mulas, S. Panero, and B. Scrosati, Electrochem. Commun. **9**, 2075 (2007).
[7] O. Mao, R. A. Dunlap, and J. R. Dahn, J. Electrochem. Soc. **146**, 405 (1999).
[8] P. P. Ferguson, A. D. W. Todd, and J. R. Dahn, Electrochem. Commun. **10**, 25 (2008).
[9] M. Gauthier, D. Mazouzi, D. Reyter, B. Lestriez, P. Moreau, D. Guyomard, L. Roué, and L. Roue, Energy Environ. Sci. **6**, 2145 (2013).
[10] P. B. Prates, A. M. Maliska, A. S. Ferreira, C. M. Poffo, Z. V. Borges, J. C. De Lima, and R. S. De Biasi, J. Appl. Phys. **118** (2015).

[11] T. D. Hatchard, J. S. Thorne, S. P. Farrell, and R. A. Dunlap, J. Phys. Condens. Matter **20**, 445205 (2008).
[12] P. P. Ferguson, D. B. Le, A. D. W. Todd, M. L. Martine, S. Trussler, M. N. Obrovac, and J. R. Dahn, J. Alloys Compd. **595**, 138 (2014).
[13] Z. Du, S. N. Ellis, R. A. Dunlap, and M. N. Obrovac, J. Electrochem. Soc. **163**, A13 (2015).
[14] L. MacEachern, R. A. Dunlap, and M. N. Obrovac, J. Electrochem. Soc. **162**, A229 (2014).
[15] S.-O. Kim and A. Manthiram, J. Mater. Chem. A **3**, 2399 (2015).
[16] P. P. Ferguson, M. L. Martine, R. A. Dunlap, and J. R. Dahn, Electrochim. Acta **54**, 4534 (2009).
[17] Z. Du, R. A. Dunlap, and M. N. Obrovac, J. Electrochem. Soc. **163**, A2011 (2016).